Effects of three-dimensional conducting structures on Resistive Wall Modes

Fabio Villone[1] , Y.Q. Liu[2]

[1]Ass. EURATOM/ENEA/CREATE, DAEIMI, Università di Cassino, Italy

[2] EURATOM/UKAEA Fusion Association, Culham Science Centre, Abingdon, UK

With contributions of:
R. Albanese, G. Ambrosino, T. Bolzonella, M. Furno Palumbo, S. Medvedev, R. Paccagnella, A. Portone, G. Rubinacci, S. Ventre

Outline

- Introduction
- The CarMa code
- Examples of application
  - Benchmarks
  - Multimodal analysis
  - Experimental validation
- ITER results
  - 3D effects on growth rates
  - "huge" computations
  - Feedback controller design & validation
- Conclusions & perspective

What are RWM?

- Linearized ideal MHD equations can describe fusion plasmas in some situations
  - In some cases predict unstable modes on inertial time scale (microseconds for typical parameters)
  - External kink is one of the most dangerous (e.g. setting beta limits in tokamaks)
  - A sufficiently close perfectly conducting wall may stabilize such mode thanks to image currents induced by plasma movements
  - Due to finite wall resistivity, image currents decay (Resistive Wall Modes) $\Rightarrow$ the mode is again unstable but on eddy currents time scale (typically milliseconds or slower)
  - Feedback active control becomes possible

How do we analyse RWM?

- Solution of a coupled problem is needed in principle
  - Plasma evolution can be described by MHD equations
  - Eddy currents equations need magneto-quasi-static electromagnetic solvers
  - Usual stability codes (MARS-F, KINX, etc.): MHD solver + a simplified treatment of wall (e.g. thin shell approximation, axisymmetric assumptions, single wall, etc.)
  - Our approach: coupling of a MHD solver (MARS-F) to describe plasma with a 3D eddy currents formulation (CARIDDI) to describe the wall $\Rightarrow$ CarMa code

3D eddy currents formulation /1

- Integral formulation assuming **J** as unknown
  - Well suited for fusion devices (only the conducting domain V_c must be meshed)
  - This formulation is at the basis of the CARIDDI code, widely used for electromagnetic computations on fusion devices
  - Volumetric conductors of arbitrary shape taken into account (no thin shell approximation nor other simplifications)
  - Electric vector potential $\mathbf{J} = \nabla \times \mathbf{T} \Rightarrow$ solenoidality of **J**
  - Non-standard two-component gauge (numerically convenient)
  - Tree-cotree decomposition of the mesh $\Rightarrow$ minimum number of discrete unknonws $\underline{I}$
  - Edge elements $\mathbf{N}_k \Rightarrow$ right continuity conditions on **J**
  - Automatic treatment of complex topologies and electrodes

3D eddy currents formulation /2

- Mathematical model
  - Eddy currents equation in the time domain
  - No magnetic materials (not a theoretical limitation: easily taken into account)
  - Resistivity tensor $\underline{\eta}$ to account for anisotropies (e.g. for "equivalent" piecewise homogeneous materials)
  - Ohm's law E = η J imposed in weak form (Galerkin approach)

- Equations:

$$\underline{\underline{\mathrm{R}}}\,\underline{\mathrm{I}} + \underline{\underline{\mathrm{L}}}\frac{d\underline{\mathrm{I}}}{dt} = -\frac{d\,\underline{\mathrm{U}}}{dt} + \underline{\underline{\mathrm{F}}}\,\underline{\mathrm{V}}$$

Magnetic vector potential due to current density representing plasma

$$R(i,j) = \int_{V_c} \nabla\times\mathbf{N}_i \cdot \underline{\underline{\eta}} \cdot \nabla\times\mathbf{N}_j\, dV$$

Electrode with potential V_j

$$U_i = \frac{\mu_0}{4\pi}\int_{V_c} \nabla\times\mathbf{N}_i \cdot \mathbf{A}_0\, dV$$

$$L(i,j) = \frac{\mu_0}{4\pi}\int_{V_c}\int_{V_c} \frac{\nabla\times\mathbf{N}_i(\mathbf{r})\cdot\nabla\times\mathbf{N}_j(\mathbf{r}')}{|\mathbf{r}-\mathbf{r}'|}\,dV\,dV'$$

$$F_{i,j} = -\int_{S_j} \nabla\times\mathbf{N}_i \cdot \hat{\mathbf{n}}\, dS$$

MHD formulation

- Single fluid linearized MHD equations

$$\rho \frac{\partial \mathbf{v}}{\partial t} = -\nabla p + \mathbf{j} \times \mathbf{B} + \mathbf{J} \times \mathbf{b}$$

$$\frac{\partial \mathbf{b}}{\partial t} = \nabla \times \left(\mathbf{v} \times \mathbf{B} \right)$$

$$\frac{\partial p}{\partial t} = -\mathbf{v} \cdot \nabla P - \Gamma P \nabla \cdot \mathbf{v}$$

$$\nabla \times \mathbf{b} = \mu_0 \mathbf{j}$$

- p, v, ρ: plasma pressure, velocity and density; Γ: specific heats ratio
- Uppercase: reference values, lowercase: first-order perturbations
- A exp(j $n\,\varphi$) dependence of the quantities is assumed in the toroidal direction φ (n : toroidal mode number)
- In the poloidal plane, Fourier decomposition is used along the poloidal angle, and a Galerkin-based finite element method is implemented on a staggered grid along the radial direction.

- Toroidal plasma flow and various kinetic effects (to simulate the damping) are presently not included in CarMa
- The MHD solver used is MARS-F

Coupling strategy

- Plasma mass is neglected
  - Good approximation if the time scale is much longer than inertial times (i.e. >> microseconds)
  - The plasma response is instantaneous and can be characterized by a response matrix to unit total normal field perturbations on coupling surface
- No plasma rotation is considered
  - Worst case analysis (moreover in ITER it is not clear if rotation will have a significant stabilizing effect)
- A coupling surface S is chosen
  - Any surface in between plasma and conducting structures
  - The plasma-wall interaction is decoupled via S

(De-)coupling surface *S* (*I*)

- The plasma (instantaneous) response to a given magnetic flux density perturbation on *S* is computed as a plasma response matrix.

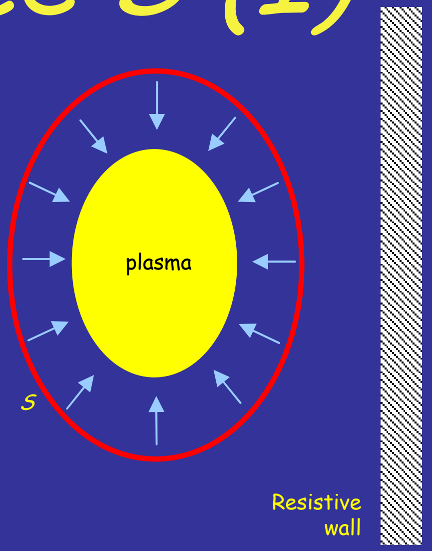

(De-)coupling surface *S* (*II*)

- The plasma (instantaneous) response to a given magnetic flux density perturbation on *S* is computed as a plasma response matrix.
- Using such plasma response matrix, the effect of 3D structures on plasma is evaluated by computing the magnetic flux density on *S* due to 3D currents.

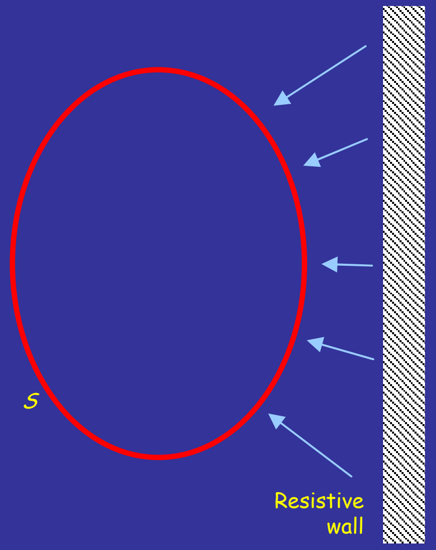

(De-)coupling surface *S* (III)

- The plasma (instantaneous) response to a given magnetic flux density perturbation on *S* is computed as a plasma response matrix.
- Using such plasma response matrix, the effect of 3D structures on plasma is evaluated by computing the magnetic flux density on *S* due to 3D currents.
- The currents induced in the 3D structures by plasma are computed via an equivalent surface current distribution on *S* providing the same magnetic field as plasma outside *S*.

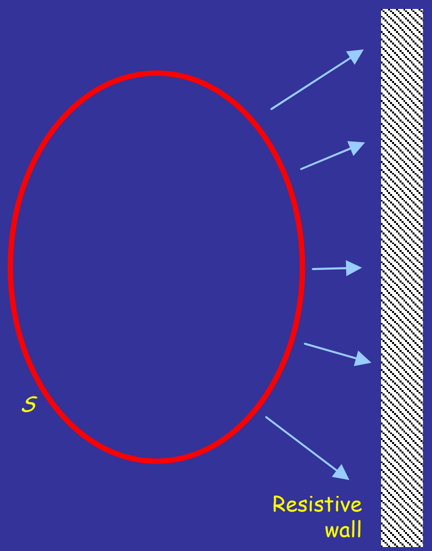

Overall model

$$\underline{\underline{R}}\,\underline{I}+\underline{\underline{L}}\frac{d\underline{I}}{dt}=-\frac{d\underline{U}}{dt}+\underline{\underline{F}}\,\underline{V}$$

Induced voltage on 3D structures

Modified inductance matrix

$$\underline{\underline{L}}^{*}\frac{d\underline{I}}{dt}+\underline{\underline{R}}\,\underline{I}=\underline{\underline{F}}\,\underline{V}$$

$$\frac{d\underline{I}}{dt}=\underline{\underline{A}}\,\underline{I}+\underline{\underline{B}}\,\underline{V}$$

Dynamical matrix

$$\underline{U}=\underline{\underline{M}}\;\underline{I}_{eq}$$

Mutual inductance matrix between 3D structures and equivalent surface currents

Matrix expressing the effect of 3D current density on plasma

$$\underline{I}_{eq}=\underline{\underline{K}}\,\underline{\underline{B}}_{En}^{-1}\,\underline{\underline{Q}}\;\underline{I}$$

Equivalent surface currents providing the same magnetic field as plasma

$N\times h$ matrix

$h\times N$ matrix

$$\underline{\underline{L}}^{*}=\underline{\underline{L}}+\underline{\underline{S}}\;\underline{\underline{Q}}$$

$h \ll N$

h DoF of magnetic field on S

N DoF of current in 3D structure

Several possible uses…

- Growth rate calculation
  - Unstable eigenvalue of the dynamical matrix
  - Standard routines (e.g. Matlab) or ad hoc computations (e.g. inverse iteration: see the following…)
  - Beta limit with 3D structures (when the system gets fictitiously stable)
- Controller design
  - state-space model (although with large dimensions and with many unstable modes)
- Time domain simulations
  - Controller validation
  - Inclusion of non-ideal power supplies (voltage/current limitations, time delays, etc.)

Benchmarks /1 (I)

- MARS-F as reference
  - Axisymmetric geometry (although with a 3D mesh)
  - stable and unstable modes with toroidal mode number $n = 1$
  - degenerate pairs of eigenvalues (modes shifted of 90° toroidally)

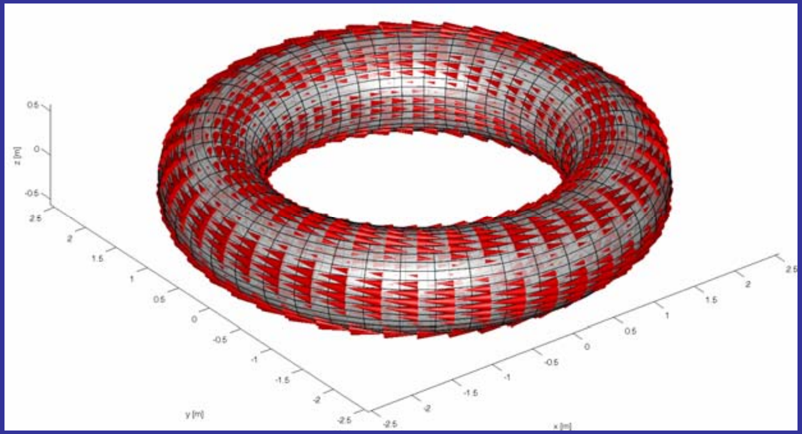

	MARS-F	CarMa, Coupling surface S_1	CarMa, Coupling surface S_2
Unstable eigenvalue (s^{-1})	292.7	291.2	293.3
Stable eigenvalue #1 (s^{-1})	165.7	159.2	159.3
Stable eigenvalue #2 (s^{-1})	221.4	216.6	216.6
Stable eigenvalue #3 (s^{-1})	279.4	278.7	278.2
Stable eigenvalue #4 (s^{-1})	379.0	373.9	374.0
Stable eigenvalue #5 (s^{-1})	560.5	562.1	561.3
Stable eigenvalue #6 (s^{-1})	589.1	581.2	581.3

Benchmarks /1 (II)

- MARS-F as reference
  - Axisymmetric geometry (although with a 3D mesh)
  - stable and unstable modes with toroidal mode number $n = 1$
  - degenerate pairs of eigenvalues (modes shifted of 90° toroidally)

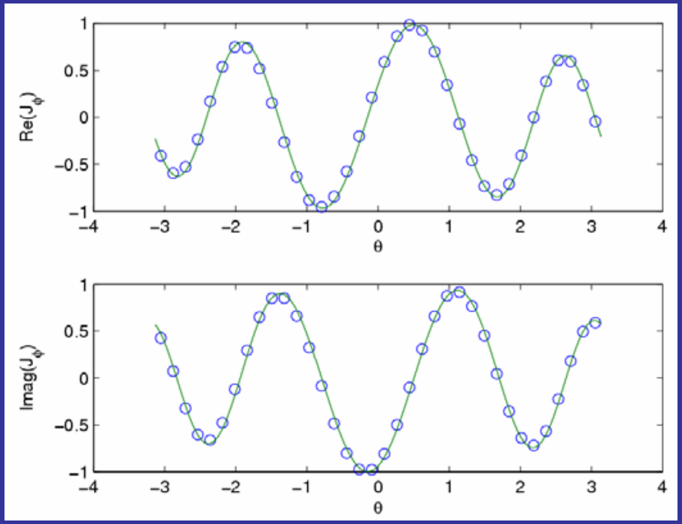

	MARS-F	CarMa, Coupling surface S_1	CarMa, Coupling surface S_2
Unstable eigenvalue (s^{-1})	292.7	291.2	293.3
Stable eigenvalue #1 (s^{-1})	165.7	159.2	159.3
Stable eigenvalue #2 (s^{-1})	221.4	216.6	216.6
Stable eigenvalue #3 (s^{-1})	279.4	278.7	278.2
Stable eigenvalue #4 (s^{-1})	379.0	373.9	374.0
Stable eigenvalue #5 (s^{-1})	560.5	562.1	561.3
Stable eigenvalue #6 (s^{-1})	589.1	581.2	581.3

Benchmarks /1 (III)

- MARS-F as reference
  - Axisymmetric geometry (although with a 3D mesh)
  - stable and unstable modes with toroidal mode number $n = 1$
  - degenerate pairs of eigenvalues (modes shifted of 90° toroidally)

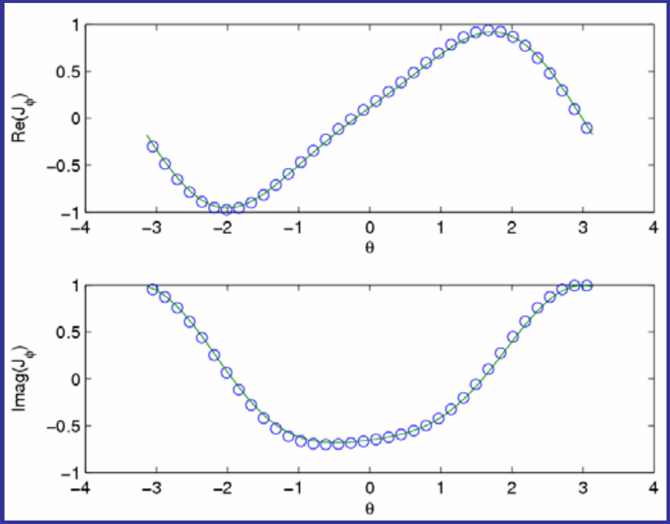

	MARS-F	CarMa, Coupling surface S_1	CarMa, Coupling surface S_2
Unstable eigenvalue (s^{-1})	292.7	291.2	293.3
Stable eigenvalue #1 (s^{-1})	165.7	159.2	159.3
Stable eigenvalue #2 (s^{-1})	221.4	216.6	216.6
Stable eigenvalue #3 (s^{-1})	279.4	278.7	278.2
Stable eigenvalue #4 (s^{-1})	379.0	373.9	374.0
Stable eigenvalue #5 (s^{-1})	560.5	562.1	561.3
Stable eigenvalue #6 (s^{-1})	589.1	581.2	581.3

Benchmarks /2

- Two different MHD codes (MARS-F, KINX) for plasma response computations
  - ITER case with axisymmetric 3D mesh
  - "Pure" MHD model benchmark (wall treated in the same way)
  - Flexibility of the approach
  - Modularity of the code

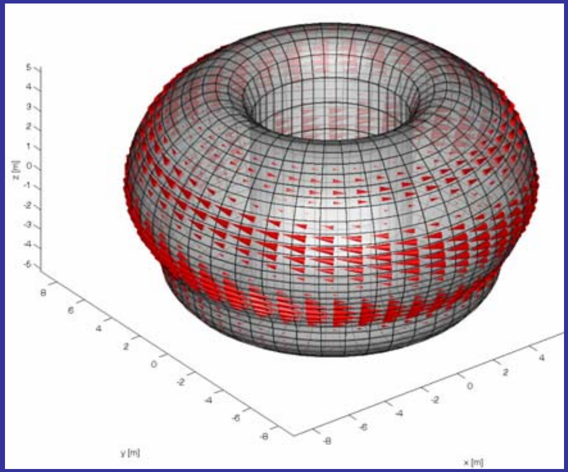

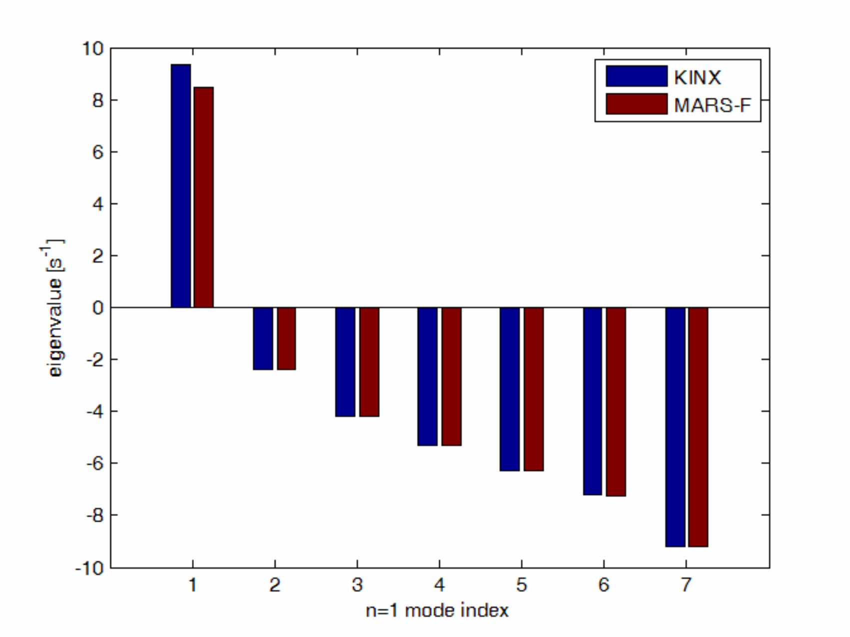

Benchmarks /3

- Theoretically sound approach
  - Independent theoretical validation on general geometry (V. Pustovitov, PPCF and this conference)
  - Analytical proof of the coupling scheme available in the cylindrical limit
  - No fitting parameters, no tuning, no normalizations
  - "Genuine" MHD computations with 3D geometries are possible

Multimodal analysis /1

- 3D structure cause multimodal coupling
  - With an axisymmetric structure linear MHD predicts that every different n evolves separately
  - A 3D structure can couple different n's even in linear MHD
- RFP's particularly suitable
  - Many unstable modes with a rich toroidal spectrum
- RFX-mod has a dedicated control system
  - 192 independently fed saddle coils
  - Selective control of non-axisymmetric modes
  - Excellent magnetic measurement coverage

Multimodal analysis /2

- RFX-mod shell with gaps
  - A small but noticeable multimodal coupling effect
  - Mode degeneracy removed

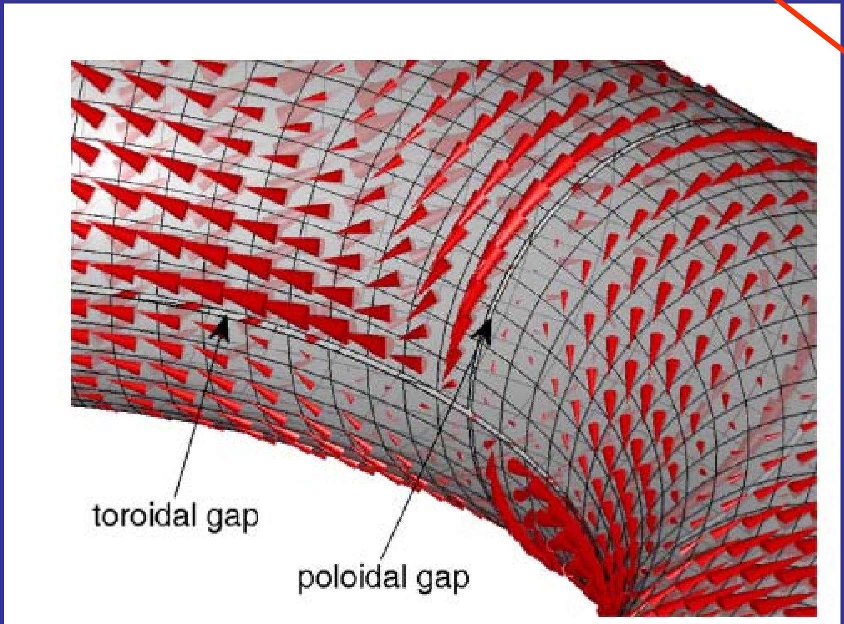

n value	CARMA monomodal	CARMA multimodal
1	<0	<0
2	0.447	0.448
	0.459	0.462
	2.40	2.33
	2.48	2.36
3	2.58	2.61
	2.62	2.64
	2.96	3.13
	3.04	3.26
4	5.46	5.63
	5.53	5.78
5	9.62	9.91
	9.73	10.2
6	17.0	17.6
	17.2	18.2

Multimodal analysis /2

- RFPs have multiple unstable RWMs
  - Even with the same *n* value
  - This corresponds to positive *n* and negative *n* in the cylindrical limit

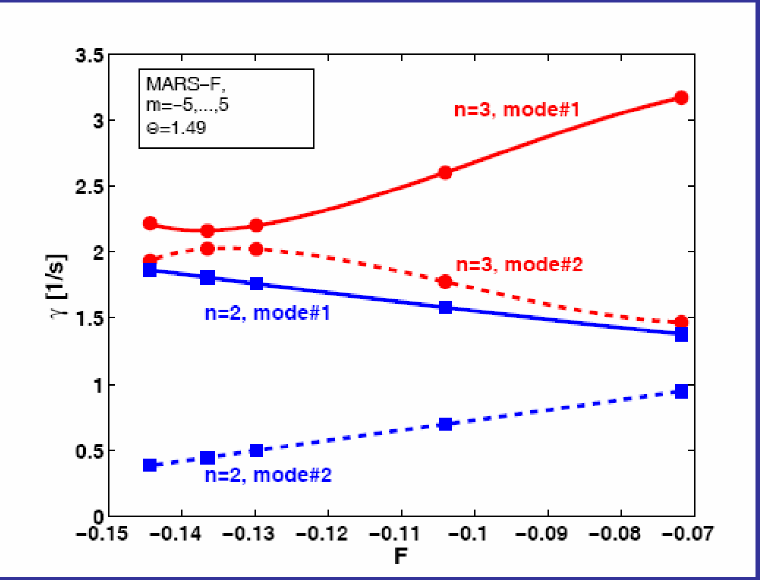

Experimental validation

Purely axisymmetric estimates of growth rates are largely underestimated

3D effects are important on growth rate!

	Equilibrium A				Equilibrium B			
	ETAW	MARSF	CarMa	Exp.	ETAW	MARSF	CarMa	Exp.
n=1	0.909	<0	<0	<0	<0	<0	<0	<0
n=2	1.56 1.82	0.780 1.29	0.869 0.931 1.67 1.81	N.A.	<0 2.45	0.434 1.81	0.448 0.462 2.33 2.36	N.A.
n=3	0.727 3.09	1.10 2.71	1.37 1.40 3.69 3.78	N.A.	1.82 1.90	2.08 2.16	2.61 2.64 3.13 3.26	N.A.
n=4	5.27	5.07	7.30 7.48	≈6	4.09	4.04	5.63 5.78	≈4.5
n=5	8.63	8.55	12.8 13.1	≈12	6.81	6.89	9.91 10.2	≈8
n=6	14.5	14.4	22.6 23.4	≈22	11.8	11.7	17.6 18.2	≈17

3D effects are significant /1 (I)

- High level of details:
  - Double shell
  - Nested port extensions
  - Outer Triangular Support with copper cladding
  - Non-axisymmetric control coils

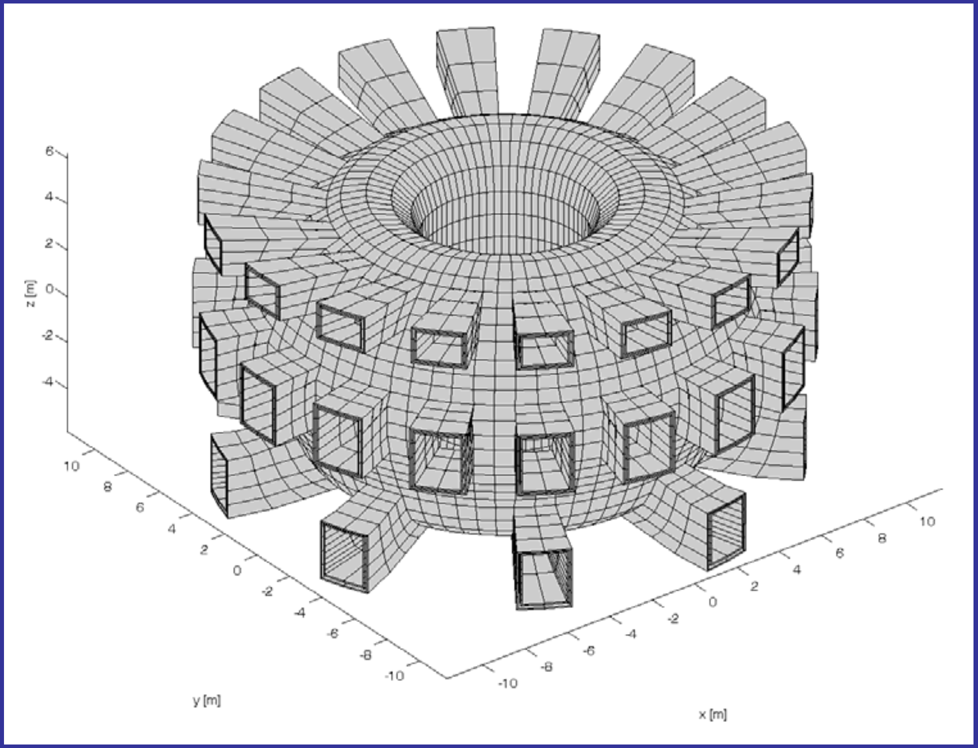

F. Villone et al., *Effects of three-dimensional conducting structures on Resistive Wall Modes*

3D effects are significant /1 (II)

- High level of details:
  - Double shell
  - Nested port extensions
  - Outer Triangular Support with copper cladding
  - Non-axisymmetric control coils

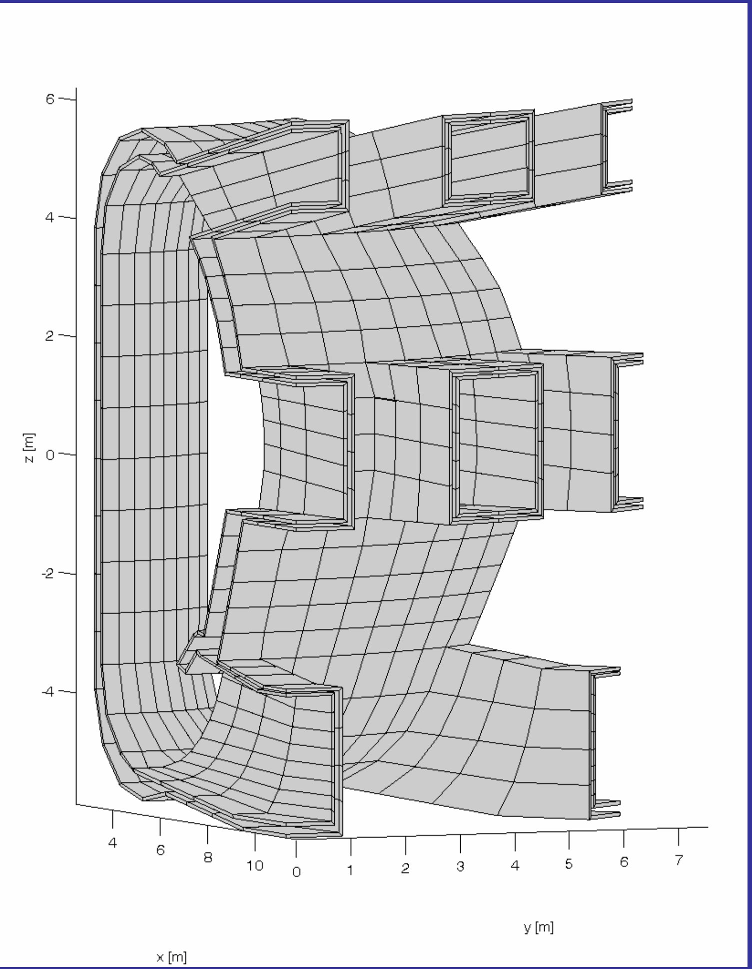

3D effects are significant /1 (III)

- High level of details:
  - Double shell
  - Nested port extensions
  - Outer Triangular Support with copper cladding
  - Non-axisymmetric control coils

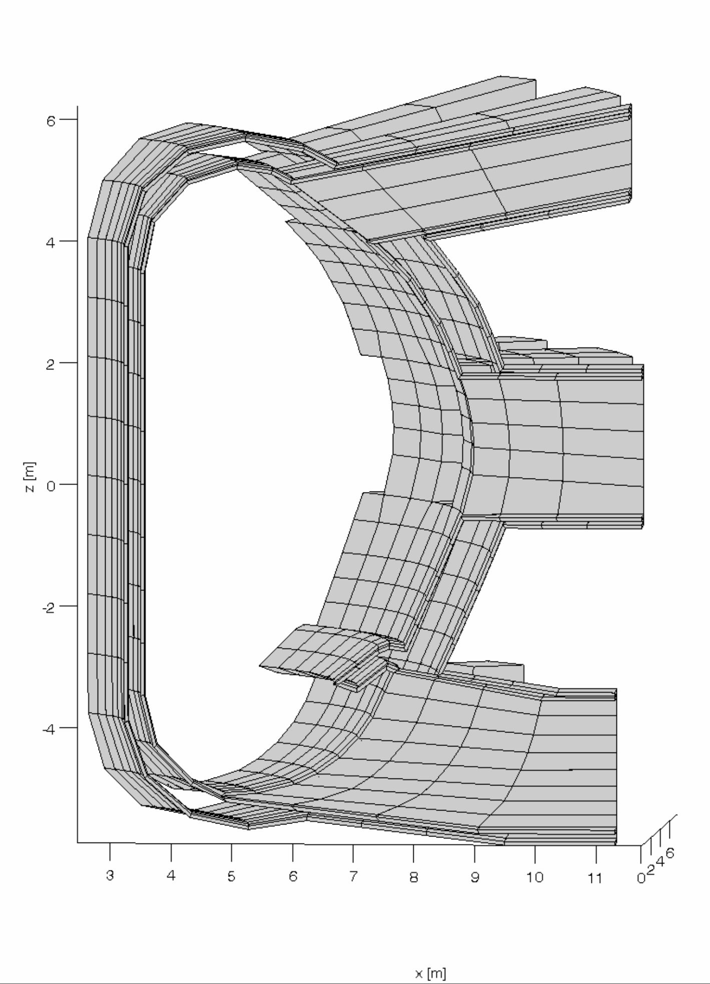

3D effects are significant /2

- Conductive patches (coarse mesh):
  - axisymmetric limit (patch with the same resistivity as vessel)
  - pure holes (simplest 3D modelling)
  - “equivalent patches”

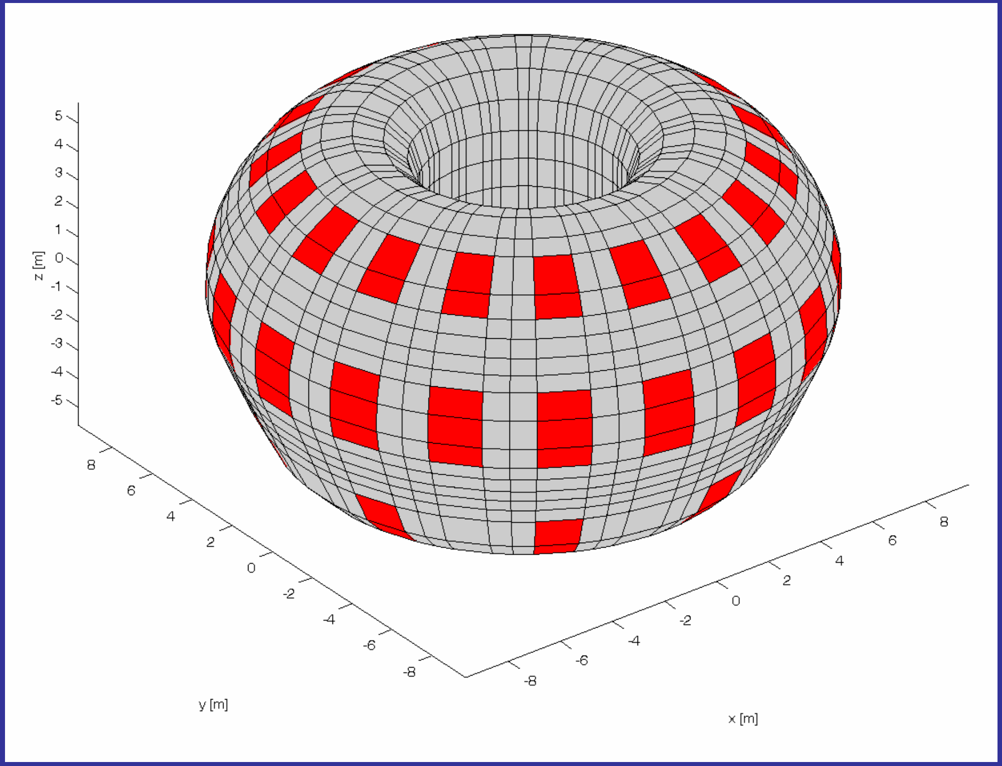

3D effects are significant /3 (I)

$n = 1$ mode

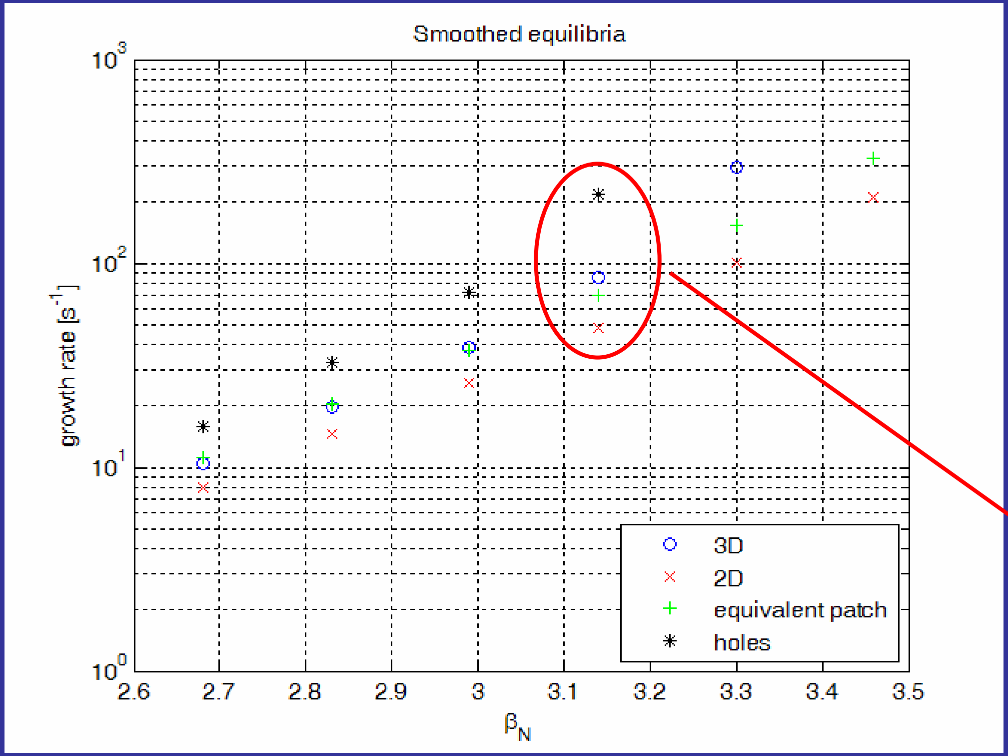

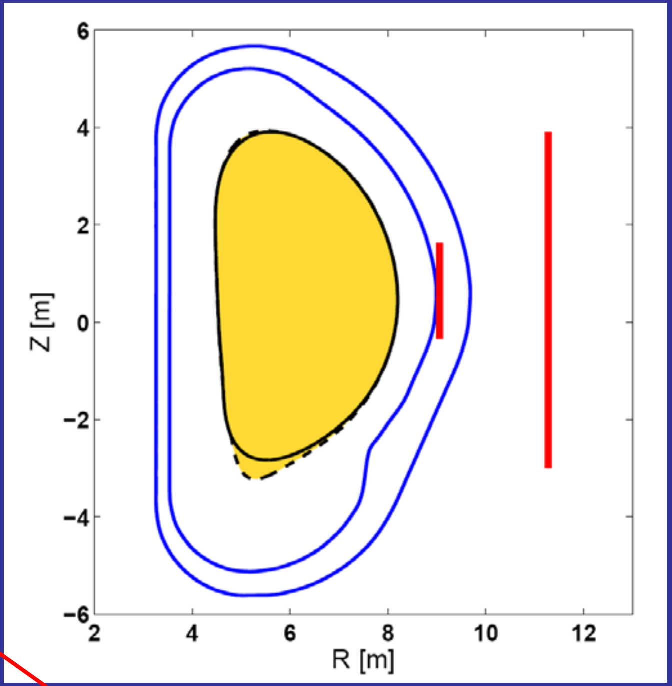

Holes are heavily pessimistic

Axisymmetric results very optimistic

3D effects are significant /3 (II)

$n = 1$ mode

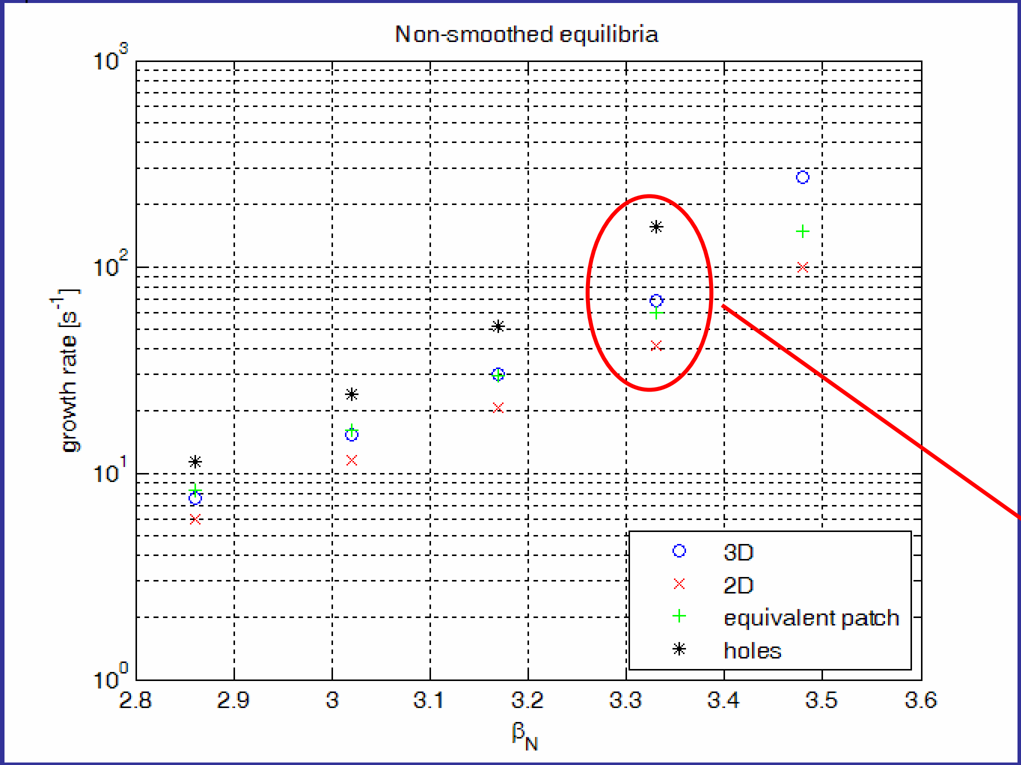

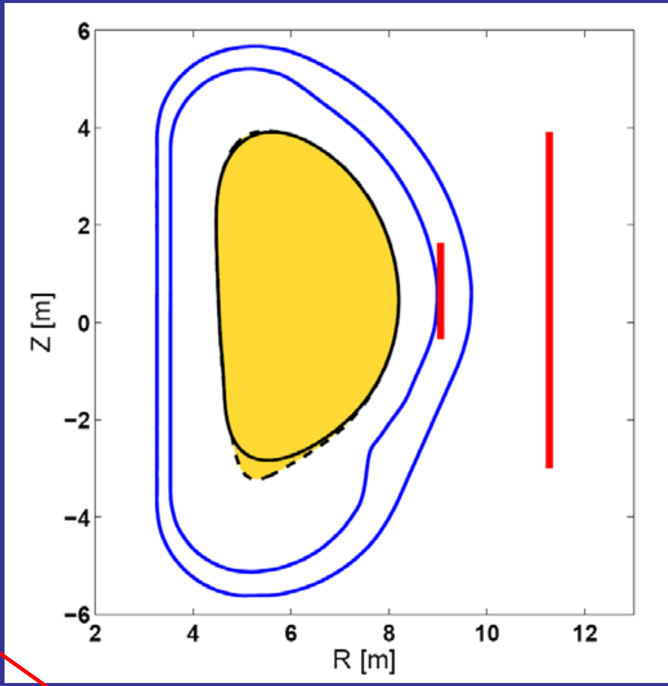

Holes are heavily pessimistic

Axisymmetric results very optimistic

3D effects are significant /4

- Why extensions are important:
  - Current density pattern corresponding to unstable eigenmode
  - current density can bypass holes using extensions

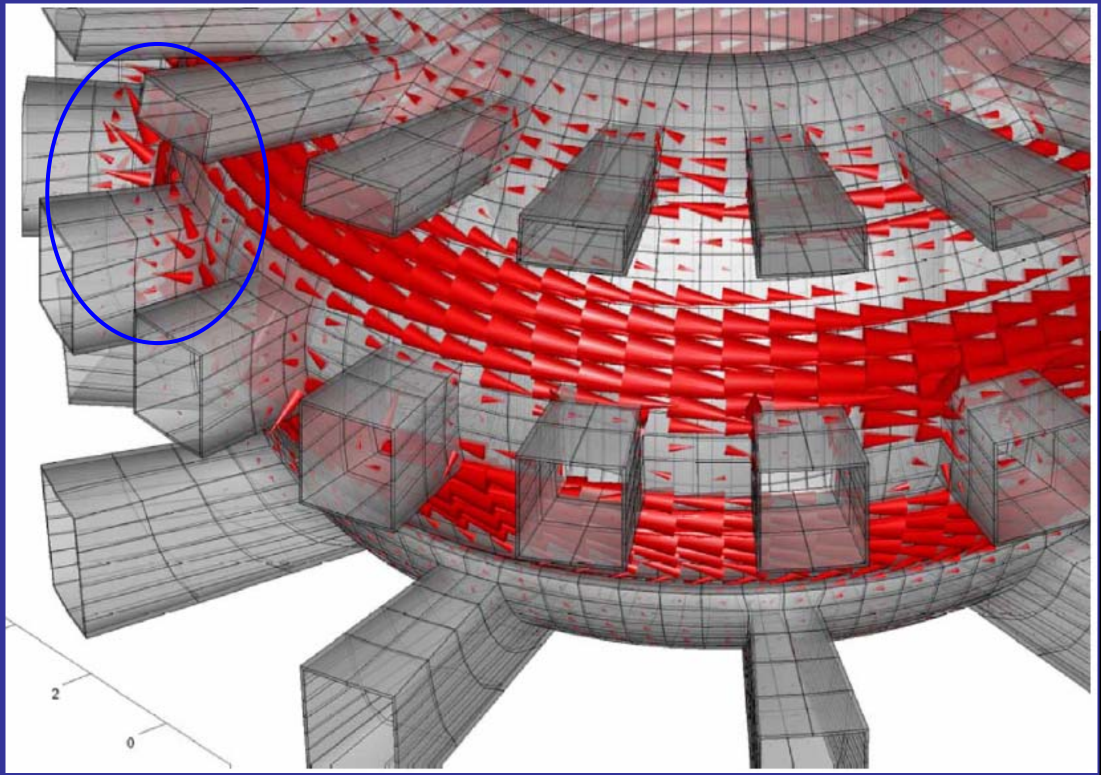

Results are reliable

- Coarse mesh with equivalent patches
  - Smoothed equilibrium with lowest beta
  - Plasma response matrices computed with KINX and MARS-F
  - n=1 modes compare well (both stable and unstable modes)

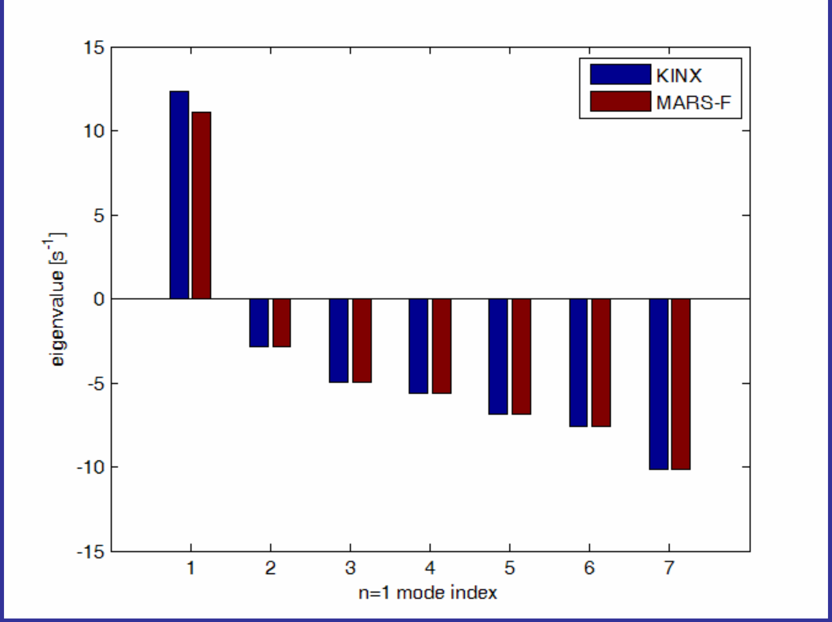

Huge computations /1

- Finding the unstable eigenvalues

$$\left(\underline{\underline{R}} + \gamma_0 \underline{\underline{L}}^*\right)\underline{I}_k = -\underline{\underline{L}}^*\underline{I}_{k-1}, \qquad \gamma_k = \gamma_0 + \frac{\underline{I}_k^T \underline{I}_{k-1}}{\underline{I}_k^T \underline{I}_k}$$

  - starting guess: γ_0 and I_0
  - tentative values γ_k and I_k at iteration k

- How do we invert this system at each k?
  - Direct methods: impractical (computational time $O(N^3)$)
  - Iterative methods: repetitive computation o $\left(\underline{\underline{R}} + \gamma_0 \underline{\underline{L}}^*\right)\underline{I}_k$ (preconditioned GMRES)
  - Fast methods to compute such product

Huge computations /2

- The issue is the computation of L I (the other terms are either sparse or factorized)
- Large parts of the discrete representation of the integral operator leading to the definition of the L matrix are numerically low rank
- A ($m1 \times m2$) submatrix B of the matrix L, representing the interactions between sources in different regions, can be described by means of a low rank QR factorization:

$$\underline{\underline{B}} \approx \underline{\underline{Q}}_B \, \underline{\underline{R}}_B$$

Q_B: $m1 \times r$, R_B: $r \times m2$, $r \ll m1, m2$

- QR factorization is obtained by using the Modified Gram-Schmidt (MGS) algorithm with an error threshold to stop the procedure

Huge computations /3

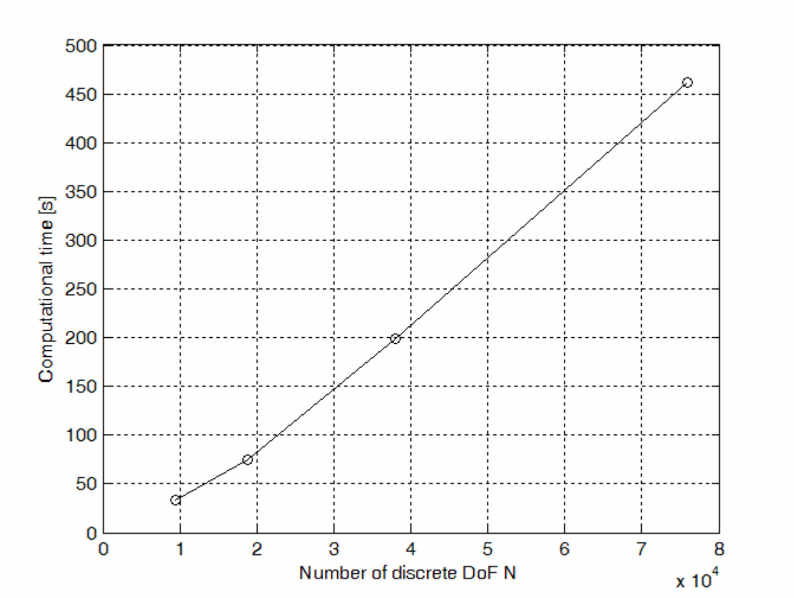

Computational time scaling almost linearly with *N*

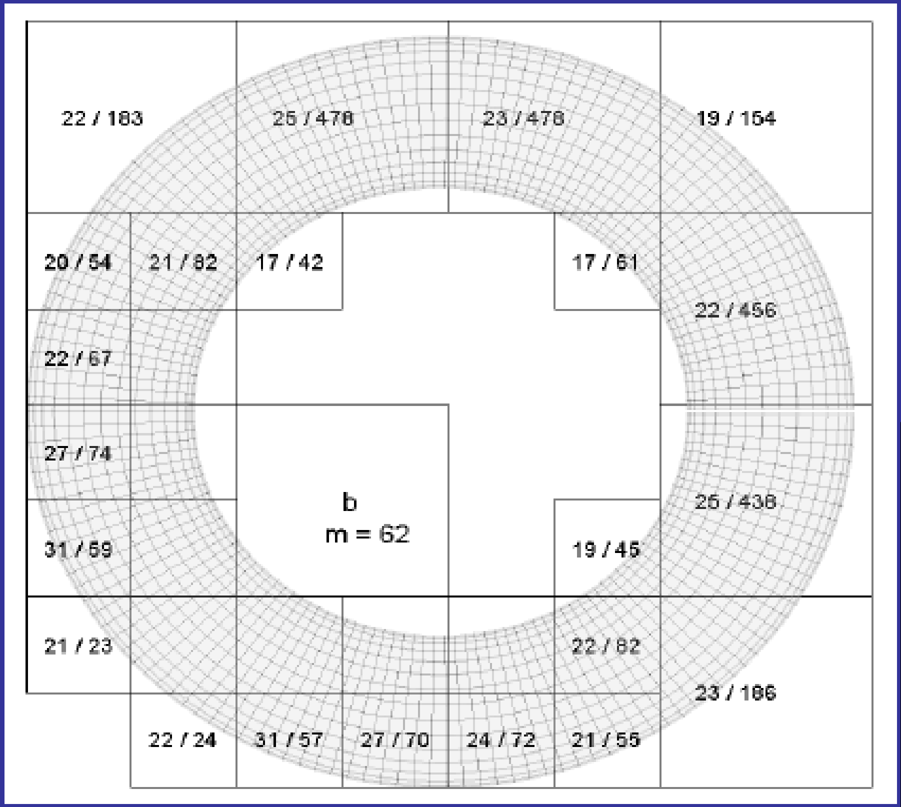

Ranks of interactions / actual dimensions

Huge computations /4

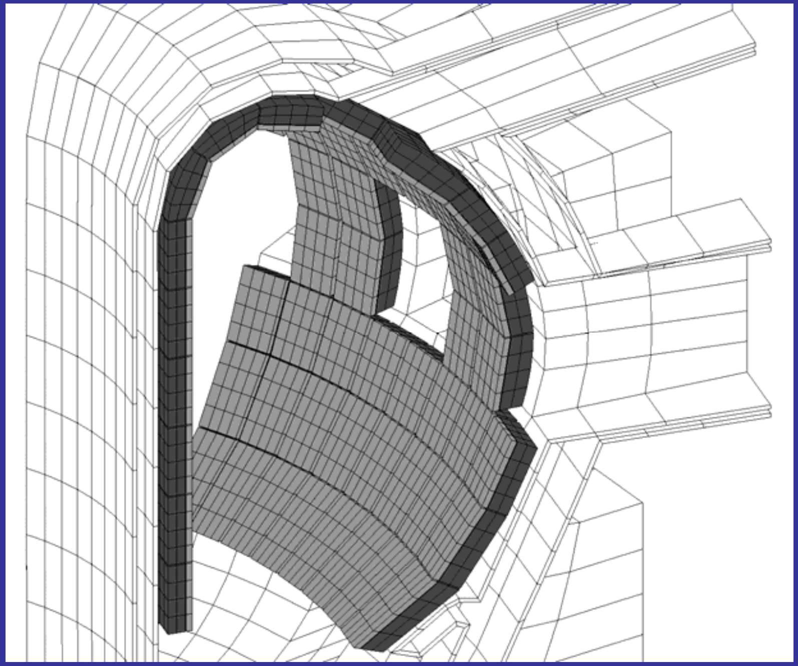

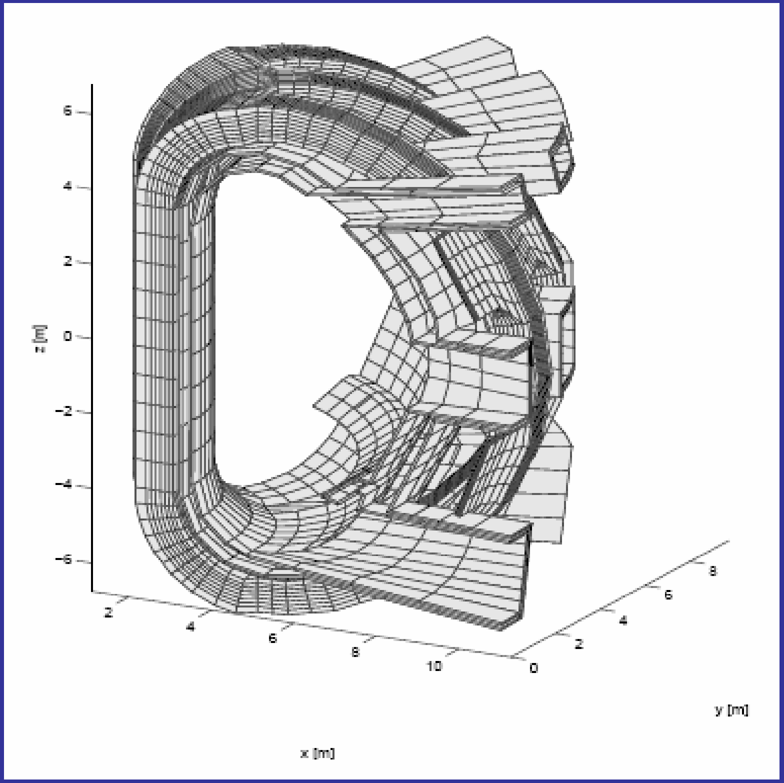

Effect of TF coil case around 2%

Effect of blanket modules around 10% (simplified modelling)

These volumetric cases (360° in the toroidal direction) cannot be analysed with standard computational tools due to memory overflow!

Best Achievable Performance /1

- Perturbations can excite unstable modes
- The voltage and currents limits of the power supplies constraint the amplitude of the maximum perturbations which can be recovered
- BAP are defined by the null controllable region:

"An initial 3D current distribution I_0 is said to be null controllable, if there exists a finite time t_f and an admissible (i.e. within voltage limits) control voltage law $V(t)$ such that the state trajectory $I(t)$ of the system satisfies $I(0)=I_0$, $I(t_f)=0$"

- The procedure for the estimation of the BAP can be modified so as to take into account also the current limits in the active coils

Best Achievable Performance /2

- Non-smoothed equilibrium with β_N = 3.17 (growth rate with 3D passive structures 30.0 s^{-1})
- 27 ELM control coil (VAC-02A option, inside vessel) can be used also for RWM control
- Voltage and current limits are much smaller if ELM control is active

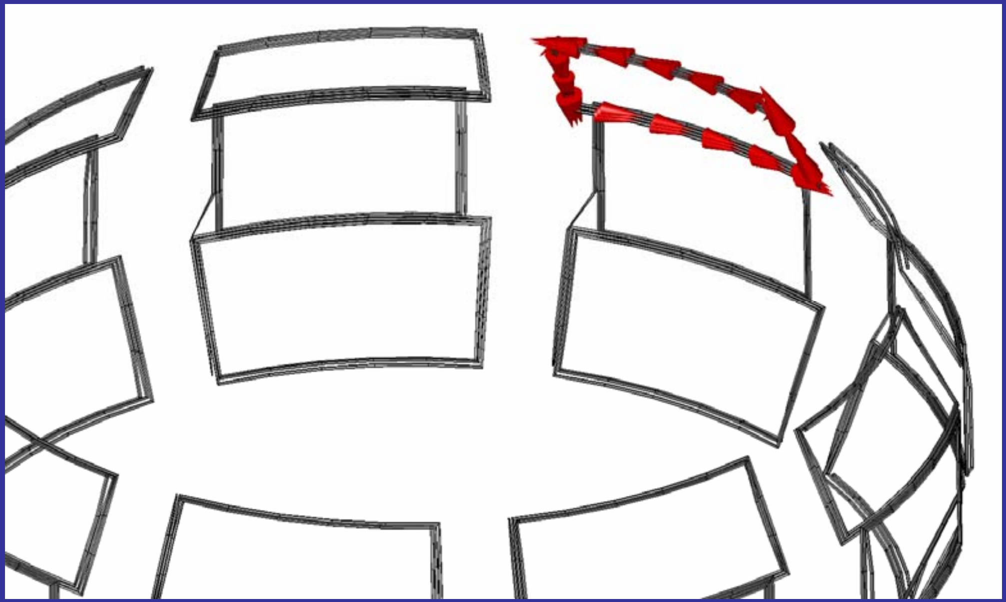

Best Achievable Performance /3 (I)

$$y_1(t) = \frac{2}{N}\sum_{k=1}^{N} B_k(t)\cos(\phi_k)$$

$$y_2(t) = \frac{2}{N}\sum_{k=1}^{N} B_k(t)\sin(\phi_k)$$

$B_k(t)$ are N=18 measurements of the vertical magnetic field in the outboard region at equally spaced toroidal angles φ_k

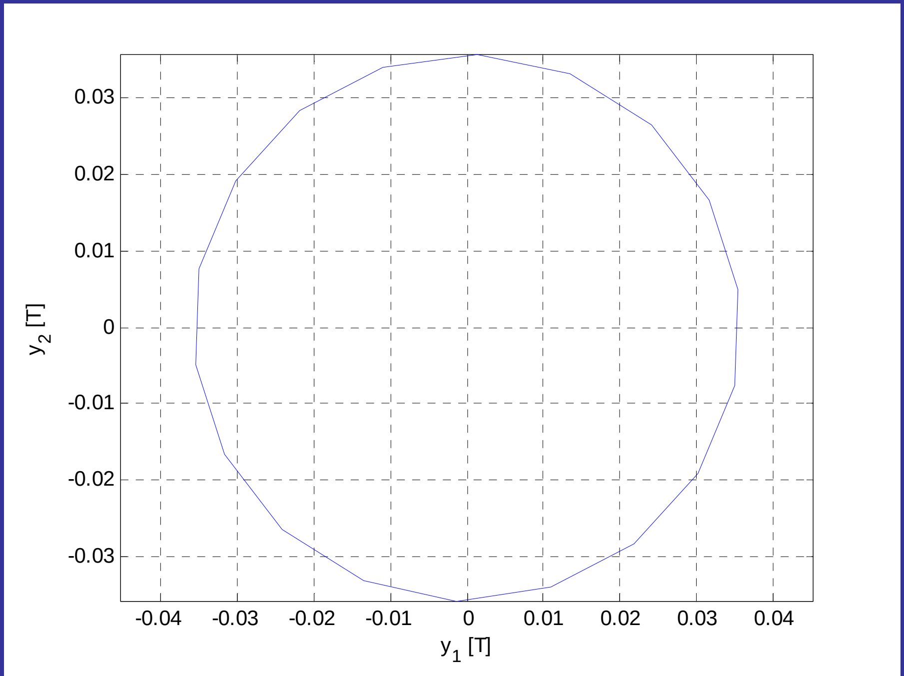

ELM control off:
current limits 20 kA

The interior of the polygon corresponds to stabilizable perturbations

The BAP is in the range of perturbations of tens of mT

Best Achievable Performance /3 (II)

$$y_1(t) = \frac{2}{N}\sum_{k=1}^{N} B_k(t)\cos(\phi_k) \qquad y_2(t) = \frac{2}{N}\sum_{k=1}^{N} B_k(t)\sin(\phi_k)$$

$B_k(t)$ are N=18 measurements of the vertical magnetic field in the outboard region at equally spaced toroidal angles φ_k

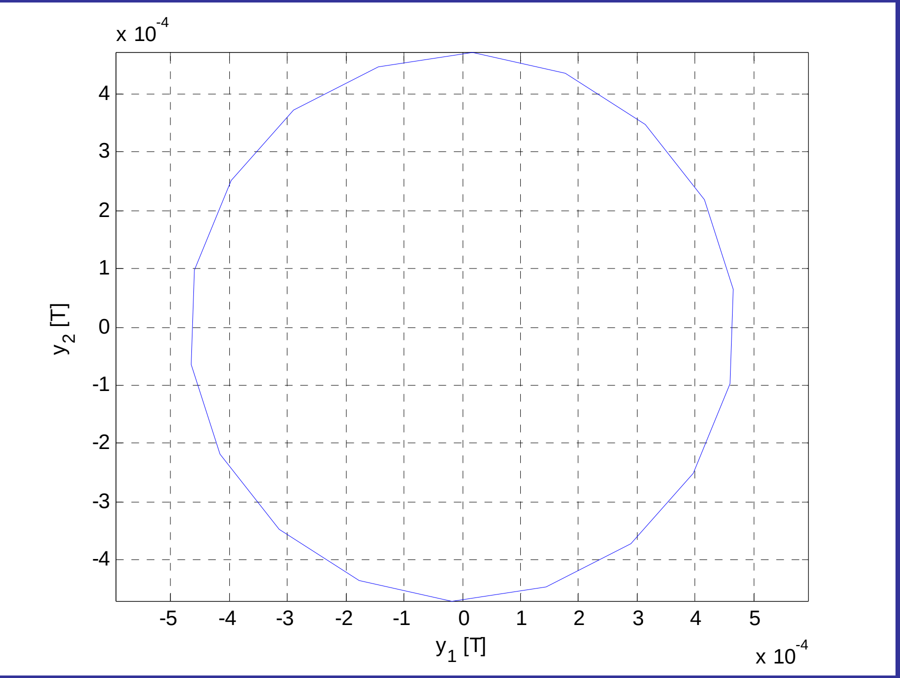

ELM control on:
current limits 250 A

The interior of the polygon corresponds to stabilizable perturbations

The BAP is in the range of perturbations of fractions of mT

Feedback controller /1

- Multivariable controller designed by using the LQG technique, based on the following requirements
  - Obtain a closed loop null controllable region as close as possible to the ideal result (BAP)
  - Allow to recover from a disturbance (initial condition on the unstable plane) as soon as possible (within current/voltage limits)
  - Avoid to generate a $n \neq 1$ magnetic field
  - Stabilize all the models with growth rates lower than reference equilibrium (i.e. lower β_N)
  - Use a balanced truncation technique to obtain a sufficiently low order controller (five)

Feedback controller /2

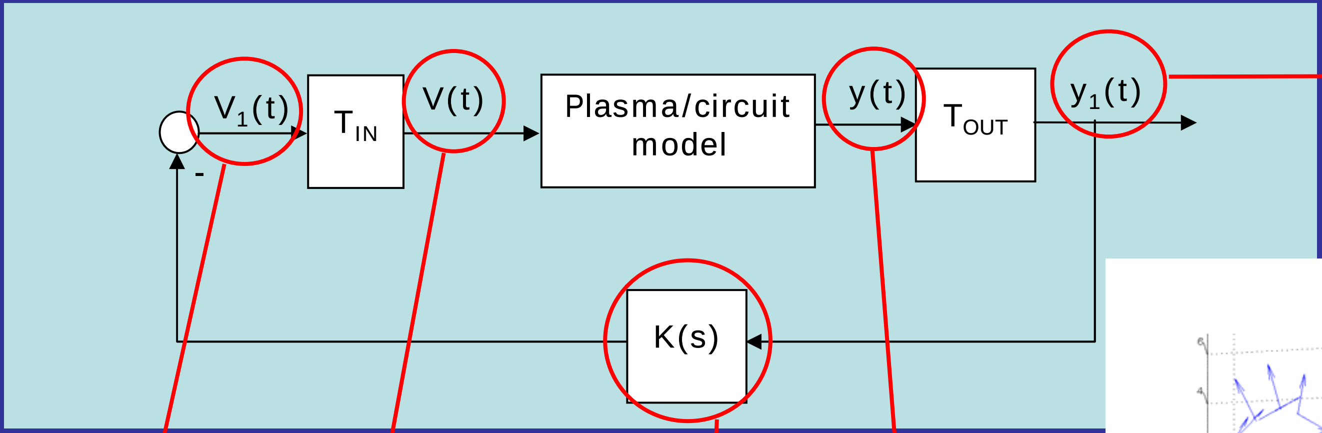

48 magnetic Fourier components

3 voltage Fourier components

27 input voltages (3 coils per 9 sectors)

144 magnetic outputs (48 measurements per 3 sectors)

RWM feedback controller

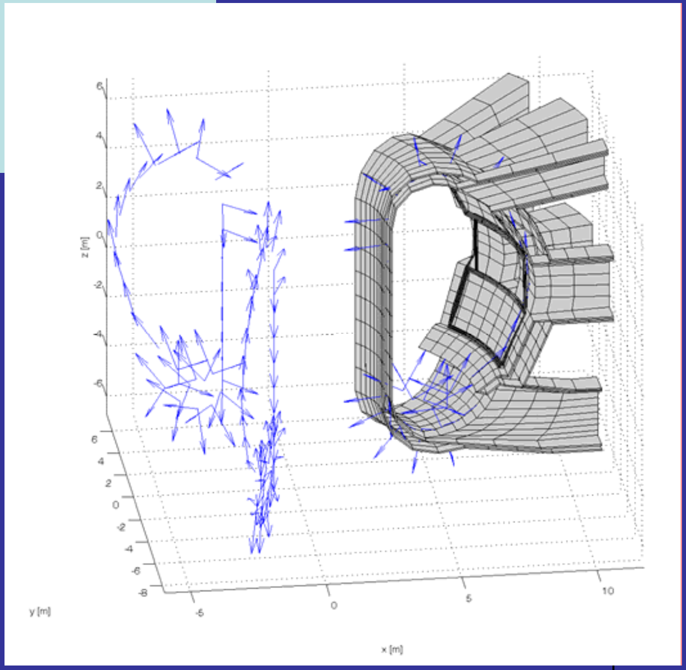

Feedback controller /3

- The maximum magnetic field displacement is of the same order of the Best Achievable Performance
- The actual limiting factor on performance is the current limit

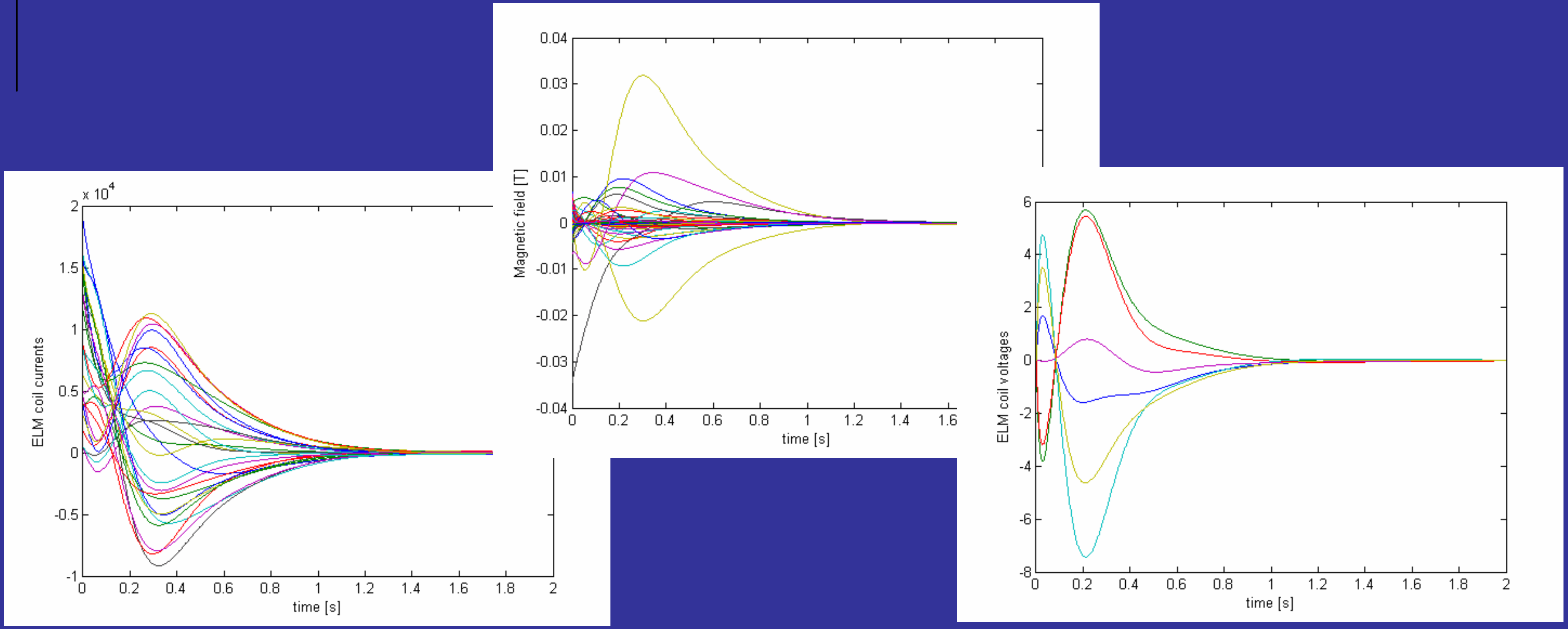

Conclusions /1

- The CarMa code can self-consistently analyse RWMs with 3D conducting structures
  - Theoretically sound (analytical proofs available)
  - Successful benchmarks on axisymmetric cases and on 3D geometries
  - Allows "pure" MHD comparisons
  - Highly modular code
  - Experimental validation on RFX
  - Multimodal modelling possible
  - Quantification of 3D effects on RFX-mod (gaps in shell) and ITER (port extensions, non axisymmetric control coils,…)
  - Huge models handling allows an unprecedented level of details in geometrical description

Conclusions /2

- Several different computations are possible
  - Growth rate computation
  - Time domain simulation
  - Feedback controller design

- 3D effects may be very significant…
  - … BUT inaccurate 3D modelling may be equally wrong!

Perspective

- Theoretically:
  - Inclusion of plasma rotation with kinetic damping models
  - Trying new coupling schemes ("backward")
  - Addition of n=0 unstable modes (VDEs + RWMs = AVDEs?)

- Experimentally:
  - Model-based controller experimental demonstration
  - Further model validation with finer geometrical description

- Practically:
  - Modelling of other existing devices
  - Latest ITER geometry (it is changing very fast…)

Some references…

F. Villone et al., *Proc. of 34th EPS Conference,* Warsaw (2007), P5.125

R. Albanese, Y. Q. Liu, A. Portone, G. Rubinacci, and F. Villone, *IEEE Trans. Magn.* 44, 1654 (2008).

A. Portone, F. Villone, Y. Q. Liu, R. Albanese, and G. Rubinacci, *Plasma Phys. Controlled Fusion* 50, 085004 (2008)

Y. Q. Liu, R. Albanese, A. Portone, G. Rubinacci, and F. Villone, *Phys. Plasmas*, 15, 072516 (2008)

F. Villone, Y. Q. Liu, R. Paccagnella, T. Bolzonella, and G. Rubinacci, *Phys. Rev. Lett.* 100, 255005 (2008)

Please contact: villone@unicas.it